

Single-atom $>$ NCS Bridging in Binuclear Complexes of Mn^{II}, Fe^{II}, Co^{II}, Ni^{II}, and Cu^{II} of Macrocyclic 20- and 22-Membered Ligands: a Spectroscopic, Crystallographic, and Molecular Mechanics Study *

Charlie Harding, Debbie McDowell, and Jane Nelson

Chemistry Department, Open University, Milton Keynes MK7 6AA

Suman Raghunathan and Clarke Stevenson

Chemistry Department, Queens University, Belfast BT9 5AG

Michael G. B. Drew and Paul C. Yates

Chemistry Department, The University, Whiteknights, Reading RG6 2AD

Using a set of macrocyclic ligands 8,12;21,25-dinitrilo-1,6,14,19-tetra-azacyclohexacos-1(26),6,8,10,13,19,22,24-octaene (L¹), 7,11;19,23-dinitrilo-1,5,13,17-tetra-azacyclotetracos-1(24),5,7,9,12,17,20,22-octaene (L²), and 7,10;18,21-diepoxy-1,5,12,16-tetra-azacyclodec-1(22),5,7,9,11,16,18,20-octaene (L³), $>$ NCS bridged binuclear complexes of all five members of the first transition series from Mn^{II} to Cu^{II} have been obtained. The observation of strong i.r. absorption below 2 000 cm⁻¹ shows that the NCS⁻ ligand adopts the rare $>$ NCS bridging mode in binuclear tetrakis- or bis-(thiocyanato) complexes of Mn^{II}, Fe^{II}, Co^{II}, and Ni^{II} with the ligand L¹ and in complexes of Co^{II} and Ni^{II} with L². With L³, a NCS-*N* link between copper(II) ions is seen, the first observation of a truly symmetric Cu-N(CS)-Cu assembly. These structures have been investigated by molecular mechanics which confirms that the steric constraints of the macrocycles are responsible for the structure variations. Magnetic susceptibility measurements show that the NCS-*N* bridge is a poor mediator of magnetic interaction between paramagnetic centres, as compared with N₃⁻-*N* or OH⁻ links. The structures of the precursor compounds [BaL¹(ClO₄)₂] and [BaL²(ClO₄)₂]·EtOH have been determined by X-ray crystallography.

Many natural binuclear sites contain a pair of transition-series ions linked by a single-atom bridge which allows the efficient transmission of magnetic interactions. This is true especially of the enzymes¹ involved in the transport and utilisation of dioxygen, such as the di-iron site in haemerythrin, or dicopper sites in haemocyanin or tyrosinase, where function is associated with the ability of the binuclear site to act as a two-electron donor.

For some time^{2,3} we have been interested in the synthesis and characterisation of binuclear complexes of macrocyclic Schiff-base ligands, where the metal ions may be bridged by such exogenous (*i.e.* non-macrocyclic) donors as OR⁻ and NCS⁻. The separation of the metal ions in the latter complexes can be inferred from the nature of the thiocyanate ligand co-ordination; thiocyanate can, in consequence, be used as a qualitative probe of internuclear separation where crystallographic information is lacking. The co-ordination modes available to NCS⁻, all of which have been observed in the binuclear systems we have studied, are listed in Table 1.

For internuclear separations in excess of *ca.* 6 Å no form of bridging is possible, and terminal -NCS or -SCN co-ordination applies, depending on the preferences of the metal ion; the *N*-donor end is selected by the relatively 'hard' class A transition-series ions, and the *S* donor by the softer class B main-group ion Pb²⁺. The internuclear separation typically⁴ associated with the commonly observed centrosymmetric di- μ -NCS-*N,S*-arrangement (mode C) was estimated at 5.6 Å, and this was borne out by our survey from the Cambridge Crystallographic Database which showed distances between 5.3 and 5.8 Å (see, for example, refs. 5-7). Where such an internuclear separation is not available, and particularly where the pair of metal ions are not identical, an unsymmetric arrangement such as mode D may be adopted, which can reduce the distance necessary for accommodation of the bridging unit³ to *ca.* 4.8 Å. The μ -NCS

bridges through only N or S (mode E) are very rare; there is one example of one bridge only (E1) with a metal-metal distance of 4.347(1) Å¹⁴ and a Pb-N-Pb angle of 109.2°. With two such bridges the metal-metal distance is much smaller and the one known structural example involving transition metals has a Ni...Ni distance of 3.28 Å. Bridging through S (mode F) is also rare and the one transition-metal example leads to an internuclear separation of 2.796 Å. In this case, however, the mode of thiocyanate co-ordination is probably determined as much by the class B nature of the acceptor ion as by the available cavity space.

Reasonably good *i.r.* diagnostics exist to distinguish terminal 'long', *i.e.* -NCS- bridging (modes C and D) and 'short', *i.e.* $>$ NCS bridging (mode E). In particular, there is now ample evidence⁸⁻¹⁰ that $\nu_{\text{asym}}(\text{NCS})$ absorption below 2 000 cm⁻¹ is to be associated with the $>$ NCS bridging mode (mode E).

The preparation of complexes of macrocyclic ligands L¹ and L² was undertaken in the hope of extending the range of single-atom $>$ NCS bridging situations, so that the properties of this bridge, for example in the mediation of magnetic interactions, could be more comprehensively studied.

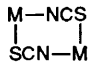
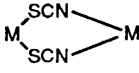
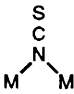
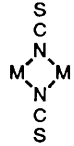
Results and Discussion

Ligands L¹ and L² were easily synthesised by [2 + 2] condensation of 2,6-diformylpyridine and the appropriate diamine on a barium(II) template in methanol as solvent. X-Ray crystallographic structure determination of the barium complexes

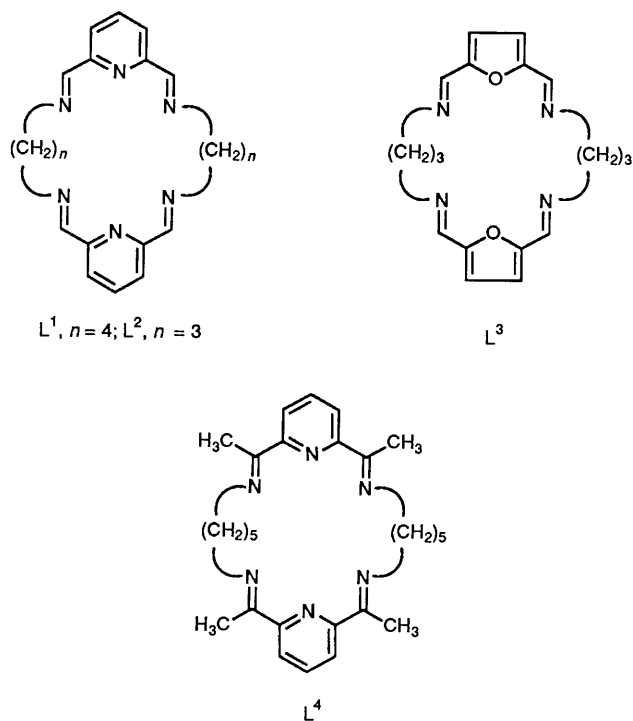
* Supplementary data available: see Instructions for Authors, *J. Chem. Soc., Dalton Trans.*, 1990, Issue 1, pp. xix-xxii.

Non-S.I. units employed: dyn = 10⁻⁵ N, cal = 4.184 J, B.M. \approx 9.27 \times 10⁻²⁴ J T⁻¹, G = 10⁻⁴ T.

Table 1. Modes of metal thiocyanate links. References are to our work. The range of M...M dimensions is taken from these structures along with others from the Cambridge Crystallographic Database

	Type	Ref.	M...M distance/Å
A	M—NCS Terminal —NCS	22	—
B	M—SCN Terminal —SCN	14, ^a	—
C	 Di-N,S-bridged centrosymmetric	3	5.3—5.8 (20 examples)
D	 Di-N,S-bridged non-centrosymmetric	3	Pb...Mn 4.857(2)
E1	 Single bridge <i>via</i> N	14	Pb...Pb 4.347(1)
E2	 Two bridges <i>via</i> N	^b	Ni...Ni 3.281(32) (1 example)
F	Two bridges <i>via</i> S	^c	Cu...Cu 2.796(8)

^a M. G. B. Drew, A. Rodgers, M. McCann, and S. M. Nelson, *J. Chem. Soc., Chem. Commun.*, 1978, 415. ^b K. R. Adam, A. J. Leong, L. F. Lindoy, B. J. McCool, A. Ekstrom, I. Liepa, P. A. Harding, K. Henrick, M. McPartlin, and P. A. Tasker, *J. Chem. Soc., Dalton Trans.*, 1987, 2537. ^c S. M. Nelson, F. S. Esho, and M. G. B. Drew, *J. Chem. Soc., Chem. Commun.*, 1981, 388.



shows in both cases that the macrocycle is folded about the metal ion so that all six nitrogen donors are within coordination distance of Ba^{2+} . The pyridine $N \cdots N$ (pyridine)

distance in $[BaL^1]^{2+}$ and $[BaL^2]^{2+}$ is, respectively, 5.59 and 5.28 Å. These distances from folded macrocycle geometries suggested to us that several types of thiocyanate bridging were possible including modes C, E1, and E2. Accordingly the viability of all three types of structure within the macrocycles has been investigated for both L^1 and L^2 *via* the method of molecular mechanics.

Molecular Mechanics Calculations.—Six different structures were modelled as we tried to assess the suitability of the macrocycles to accommodate —NCS bridges of different types. These were $M_2L(NCS)_4$ with two NCS-*N,S* bridges in a centrosymmetric arrangement (mode C), $M_2L(NCS)_4$ with two NCS-*N* bridges (mode E2) and $[M_2L(NCS)_3]^+$ with only one NCS-*N* bridge (mode E1). These calculations were carried out with both macrocycles L^1 and L^2 . Calculations were carried out using the MM2 program¹¹ in the manner described in ref. 12. Parameters were taken from ref. 11 apart from those pertaining to the thiocyanate bridges which were taken from ref. 12. In all the models the transition metal was identified as Co^{II} . Parameters used are listed in Table 2 and results are summarised in Tables 3(a) and (b). While all molecular mechanics calculations are only as good as the input parameters and there is considerable uncertainty as to the parametrisation of the bridge, we are convinced that the overall trends observed in the calculations are valid particularly as they are consistent with our experimental observations.

First, both macrocycles are too restricted to permit the *N,S*-mode of attachment of the thiocyanate ligand. Both minimised $[Co_2L(NCS)_4]$ structures of this type contain $Co \cdots Co$ distances of less than 4.0 Å which is at least 1.0 Å less than any known structure containing a NCS-*N,S* bridge. While the steric

energies are quite low (though considerably higher than for the NCS-*N* bridges), this is achieved by severe distortion of the octahedral geometry around the metal which occurred only because weak force constants were allocated to internal angles at the metal.

Of the other four structures, it is clear that the single thiocyanate-*N* bridge is considerably more stable with the 22-membered macrocycle L¹ than with the smaller 20-membered

macrocycle L². Indeed it seems unlikely that the singly bridged structure could be formed with L².

For these structures of [Co₂L(NCS)₃]⁺ an ideal Co-N-Co angle of 100° was included together with a force constant for *k_b* of 0.400 mdyn Å⁻¹ rad⁻¹ and for L² this produced after minimisation of steric energy (to 8.86 kcal mol⁻¹) a structure in which the Co-N-Co angle had changed to 83.8° and the Co...Co distance to 2.94 Å. This result seemed unlikely as it could suggest a weak metal-metal interaction. Similar calculations of L¹ showed that the proposed 100° angle could be easily accommodated. When an angle of 100° was imposed upon the L² structure (by including a strong force constant for the angle), the structure minimised to an energy of 13.83 kcal mol⁻¹ with an M...M distance of 3.29 Å. We conclude that the singly bridged structure (mode E1) is less likely for macrocycle L² than for macrocycle L¹.

On the other hand for the double thiocyanate-*N* bridge both structures have similar energies and geometries. These results are referred to below in the discussion of the experimental results.

For the two L¹ structures with NCS-*N* bridges we attempted to find the best fit for metal ions within the L¹ macrocycle. Using our published method¹³ we fixed all six M-N bonds at a particular length (by giving the bond a high force constant of 99.0 mdyn Å⁻¹) and allowed the macrocycle conformation to minimise. This was repeated for a range of bond lengths to the values given in Table 3(b). For both the single and double bridge it was found that the best fit was for M-N bonds of ca. 2.20 Å. There was little difference between the minimum position in the two cases, so it appears that our calculations cannot explain a dependence of structure on cationic radius alone.

Barium Complexes: Discussion of the Structure.—In both structures the barium atom is encapsulated within the macrocycle and bonded to all six nitrogen atoms (Figures 1 and 2). In addition the barium atom is bonded to a mix of oxygen atoms in rather different ways in the two structures.

In [BaL¹(ClO₄)₂] (1) the Ba-N distances range from 2.803(20) to 2.936(17) Å. In addition the metal ion is chelated to the ordered perchlorate ion [2.976(17) and 2.903(18) Å] and bonded to either of two oxygen atoms of the second perchlorate which is disordered. The co-ordination number of the barium atom is therefore nine. In [BaL²(ClO₄)₂]·EtOH (14) the Ba-N distances range from 2.835(16) to 3.036(18) Å. In addition the ion is chelated to two perchlorates at distances of 2.943(17)—3.061(16) Å and the oxygen atom of the ethanol solvent at

Table 2. Force-field parameters

(a) Bond stretching

	<i>k_m</i> /mdyn Å ⁻¹	<i>r₀</i> /Å
Co-S	1.00	2.65
Co-N(macrocycle)	1.00	2.05 ^a
Co-N(thiocyanate)	1.00	2.05 ^a
S-C	3.21	1.70

(b) Angle bending

	<i>k_b</i> /mdyn Å ⁻¹ rad ⁻²	θ ₀ /°
Co-N-C (macrocycle)	0.550	121.13
Co-N-C (thiocyanate terminal and N,S bridges)	0.450	180.00
Co-N-C (thiocyanate- <i>N</i> bridge)	0.300	120.00
Co-S-C (bridging thiocyanate)	0.500	90.00
S-C-N	1.500	180.00
N-Co-N (within macrocycle)	0.030	72.00, 144.00
N-Co-N ^a (six-co-ordinate structures)	0.030	90.00, 180.00
N-Co-N ^a (five-co-ordinate structures)	0.010	90.00, 180.00
Co-N-Co (single bridge)	0.400	100.00 ^b
Co-N-Co (double bridge)	0.300	100.00 ^c
N-Co-S	0.030	90.00
Co-S-C	0.500	90.00

(c) Torsional terms for i-j-k-l angles

Force constants for angles with atom j or k = Co were set to 0. Angles with i or l = Co were given parameters equivalent to those for i or l = C(sp³)

(d) Non-bonded parameters

Atom	<i>r^a</i> /Å	ε/kcal mol ⁻¹
Co	2.35	1.65

^a Nomenclature from ref. 11. Parameters not listed here are included within the MM2 program. ^b Estimate taken from ref. 3. ^c Estimates taken from structures in ref. 34 and footnote b of Table 1.

Table 3. Results of molecular mechanics calculations (a) and variations of M-N bond lengths against steric energy (b)

Compound	Bridge type	(a)		(b)		
		Energy/kcal mol ⁻¹	M...M/Å	M-N/Å	Energy/kcal mol ⁻¹	
					[M ₂ L ¹ (NCS) ₃] ⁺	[M ₂ L ¹ (NCS) ₄]
[M ₂ L ¹ (NCS) ₄]	Two NCS- <i>N</i>	10.66	3.30		E2	E1
[M ₂ L ² (NCS) ₄]	Two NCS- <i>N</i>	10.24	3.24	1.80	29.71	40.93
[M ₂ L ¹ (NCS) ₃] ⁺	One NCS- <i>N</i>	7.48	3.66*	1.90	21.13	25.62
[M ₂ L ² (NCS) ₃] ⁺	One NCS- <i>N</i> (i)	8.86	2.94*	2.00	14.67	16.88
	(ii)	13.83	3.29	2.10	9.15	12.65
[M ₂ L ¹ (NCS) ₄]	Two NCS- <i>N,S</i>	38.52	3.59	2.20	7.48	12.37
[M ₂ L ² (NCS) ₄]	Two NCS- <i>N,S</i>	32.62	3.47	2.30	8.42	12.97
				2.40	10.93	16.39
				2.50	14.86	21.34

* There are several possible conformations for these two compounds with for example the terminal and bridging thiocyanates on different sides of the molecules. However, we were unable to find any other conformations with an energy of less than 15 kcal mol⁻¹. All conformations led to values for the M...M distance that were similar to those in the table.

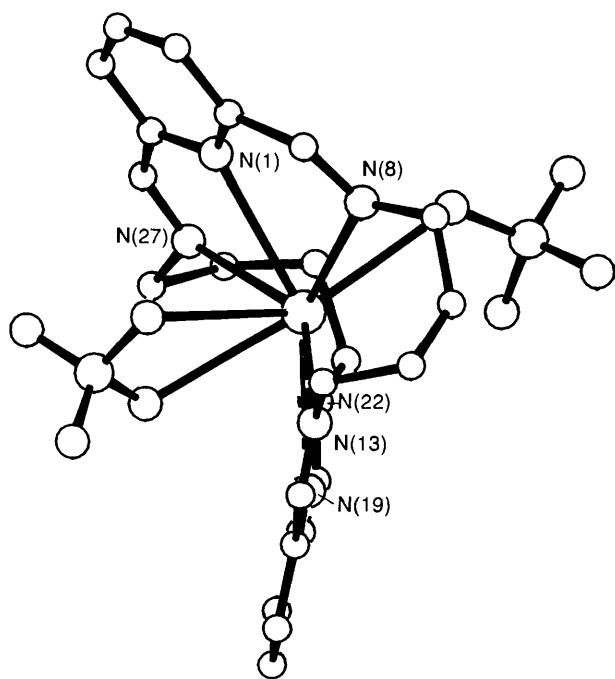


Figure 1. Crystal structure of $[\text{BaL}^1(\text{ClO}_4)_2]$ (1)

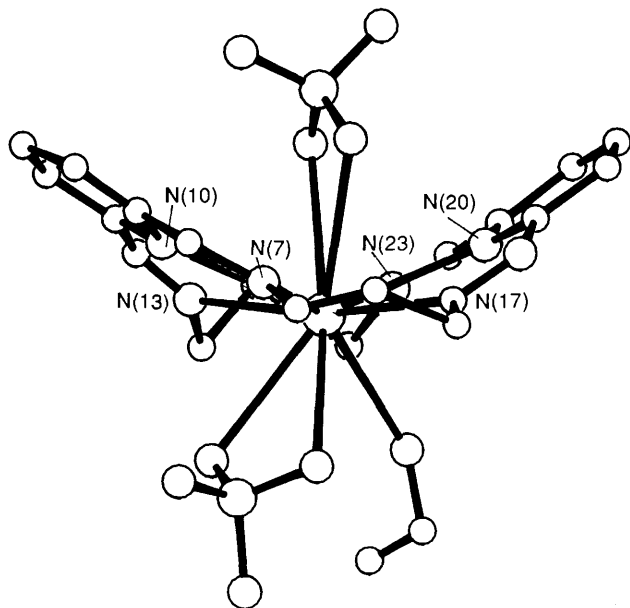


Figure 2. Crystal structure of $[\text{BaL}^2(\text{ClO}_4)_2] \cdot \text{EtOH}$ (14)

2.855(20) Å. The metal atom therefore has a co-ordination number of 11.

The shape of the macrocycle in complex (14) is of the U form with the two pyridine rings tilted to each other at an angle of 73.4° (Figure 2). However the shape of the macrocycle in (1) is not easy to define. The angle between the two pyridine rings is 63.5° but this is not just a tilt to make the U shape of (14); in addition the pyridine rings are twisted around the Ba–N axes relative to one another.

Transmetallations.—Binuclear transition-series complexes of L^1 and L^2 were prepared mainly as tetrakis- or bis-(thiocyanato) complexes (Table 4) by transmetallation in the presence of the appropriate quantity of thiocyanate ion. A number of other single-atom bridged species, M_2X_nL , where $X = \text{OH}^-$, OMe^- ,

or N_3^- were also synthesised for the purpose of comparison. Analytical and selected i.r. spectroscopic data for these compounds are listed in Table 4.

In the thiocyanate series the i.r. criterion demonstrates the wide occurrence of the single-atom $>\text{NCS}$ bridges (modes E1 and E2). Where $L = L^1$, this $M-\text{N}(\text{CS})-M$ assembly exists for $M = \text{Mn}^{\text{II}}$, Fe^{II} , Co^{II} , and Ni^{II} , but is not observed for $M = \text{Zn}^{\text{II}}$ or Cu^{II} , although a single-atom bridge is present in the dicopper(II) μ -hydroxo L^1 complex (12). Examination of the $\nu_{\text{asym}}(\text{NCS})$ absorption of dicopper(II) complexes (9) and (10) suggested the possibility of a 1,3-NCS-*N,S* bridge between the relatively small copper(II) ions co-ordinated within this 22-membered macrocycle. Our molecular mechanics calculations make this seem unlikely and it may be that such bridges connect pairs of copper ions co-ordinated by different macrocycles, an intermolecular bridge, according to the formulation given. In the case of the dizinc(II) complex (13), the pair of $\nu_{\text{asym}}(\text{NCS})$ i.r. absorptions at 2070 and 2060 cm^{-1} indicates terminal N co-ordination of all four NCS⁻ ligands.

Using the structurally characterised compound (3) as calibrant, the relative intensity of the i.r. absorption at $< 2000 \text{ cm}^{-1}$ indicates the presence of two $>\text{NCS}$ bridges in (2), but only one such bridge in the other L^1 complexes (4)–(6) and (8). For (4) and (5) the observation of a broad intense band around 2050 cm^{-1} suggests that unco-ordinated thiocyanate ion is also present, and the electronic spectrum of (5) (see later) supports this idea. (Unfortunately the tetrathiocyanato complexes have insufficient solubility for conductivity measurements.) The remaining strong absorption at 2080 cm^{-1} , characteristic of terminal $-\text{NCS}$ co-ordination, completes the $\nu_{\text{asym}}(\text{NCS})$ spectrum of (4) and (5). It thus appears likely that there are two terminal, one N-only bridged, and one ionic thiocyanate in these complexes. The proposed structure of $[\text{M}_2L^1(\text{NCS})_3]^+$ is shown in Figure 3. Several different conformations were modelled, some with terminal thiocyanates on different sides of the macrocycle, but the conformation shown had much the lower energy. The previous example¹⁴ of a structure in this category $[\text{Pb}_2L^4(\text{NCS})_3]^+$ had the terminal thiocyanates on the opposite sides to the bridging thiocyanate, but this could be due to steric restraints in the larger macrocycle and/or the large size of the Pb atom.

An interesting compound whose isolation confirms the preference of the Co_2L^1 assembly for a single $>\text{NCS}$ bridge is the monothiocyanate triperchlorate (6). This crystallises out nicely as the tetrakis(acetonitrile) solvate, but readily loses solvent in air, and we were unable to obtain a suitable data set, even when the crystal was sealed in an atmosphere of solvent, before decomposition occurred. With solvent loss, the colour changes from the red-brown typical of six-co-ordinate Co^{II} in this environment to a dark olive-green suggestive¹⁵ of five-co-ordinate square-pyramidal Co^{II} . With the addition of a co-ordinating solvent such as dimethylformamide (dmf) the red-brown colour is restored. [Similarity of the electronic spectrum of this green form of (6) with that of (5) supports the suggestion that one NCS⁻ ion in (5) is unco-ordinated.]

The only di-NCS-*N* bridged L^1 complex (2) presumably has the parallel-planar macrocyclic configuration (Figure 4) established for (3) by X-ray crystallographic structure determination. This minimised structure is equivalent to that recently established¹⁶ for (7), where the $\text{Co} \cdots \text{Co}$ distance is 3.41 Å. Compound (8) presumably adopts some variant of conformation E, with all four thiocyanate ligands co-ordinated.

So, to summarise, the co-ordination mode adapts to alteration of internuclear separation consequent on change of ionic radius in the series Mn^{II} to Zn^{II} as follows. With the largest ion, Mn^{2+} , a pair of $>\text{NCS}$ bridges allied with the parallel-planar macrocyclic conformation (Figure 4) is adopted. With the somewhat smaller Fe^{2+} and Co^{2+} ions, the U-shaped macrocyclic

Table 4. Analytical and i.r. spectroscopic data for complexes of L¹, L², and L³

Complex	Colour	Analysis ^a /%			$\Lambda^{b/S}$ cm ² mol ⁻¹	$\nu_{\text{asym}}(\text{NCS}^-)$ or $\nu(\text{N}_3^-)$	$\nu(\text{C}=\text{N})$	$\nu(\text{OMe}^-)$, $\nu(\text{ClO}_4^-)$, or $\nu(\text{BPh}_4^-)$
		N	C	H				
(1) [BaL ¹ (ClO ₄) ₂]	White	11.9 (11.8)	37.2 (37.2)	3.7 (3.7)	287		1 648m, 1 635m	1 130, 1 100, 960br,s 635, 630, 622ms
(2) [Mn ₂ L ¹ (NCS) ₄]	Yellow	19.9 (19.5)	43.8 (43.6)	3.9 (3.7)	c	2 070s, 1 965vs	1 638m	
(3) [Mn ₂ L ¹ (OMe)(NCS) ₃]	Orange-brown	18.0 (18.2)	45.0 (45.2)	4.1 (4.4)	c	2 065vs, 2 005ms	1 643m	2 784mw
(4) [Fe ₂ L ¹ (NCS) ₄ ·H ₂ O]	Red-brown	19.1 (19.0)	42.3 (42.4)	3.8 (3.8)	c	2 080s, 2 045vs, 1 960ms	1 632m	
(5) [Co ₂ L ¹ (NCS) ₄]	Bottle-green	19.4 (19.4)	43.2 (43.2)	3.6 (3.6)	c	2 080 (sh), 2 055vs, 1 960ms	1 633m	
(6) [Co ₂ L ¹ (NCS)(MeCN) ₄ - (ClO ₄) ₃]	Red-brown	14.8 (15.2)	36.2 (36.7)	3.6 (3.8)	c	1 996s	1 632m	1 100br,s 630, 625ms
(7) [Co ₂ L ¹ (N ₃) ₂ (MeCN) ₂ - (ClO ₄) ₂]	Red-brown	23.2 (22.9)	36.3 (36.4)	3.7 (3.8)	349	2 070vs, 1 355m ^d	1 628m	1 100br,s, 632 (sh), 628ms
(8) [Ni ₂ L ¹ (NCS) ₄ ·H ₂ O]	Lime green	19.1 (19.1)	42.3 (42.6)	3.7 (3.7)	c	2 090s, 2 070vs, 1 965ms	1 632m	
(9) [Cu ₂ L ¹ (NCS) ₄]	Bright green	18.8 (19.0)	42.2 (42.3)	3.6 (3.6)	c	2 105ms (sh), 2 085s	1 630m	
(10) [Cu ₂ L ¹ (NCS) ₂ (ClO ₄) ₂]	Green	13.9 (13.7)	35.3 (35.3)	3.2 (3.2)	279	2 100s	1 630m	1 109, 1 055vs, 630, 625ms
(11) [Cu ₂ L ¹ (N ₃) ₂ (ClO ₄) ₂]	Green	21.1 (21.4)	33.6 (33.7)	3.3 (3.3)	349	2 090 (sh), 2 070vs, 1 348m ^d	1 631mw	1 100vs, 628ms
(12) [Cu ₂ L ¹ (OH)(ClO ₄) ₃]	Blue-green	10.0 (10.3)	32.8 (32.3)	3.3 (3.3)	386		1 635mw	1 110, 1 065vs, 632, 628ms
(13) [Zn ₂ L ¹ (NCS) ₄]	White	18.8 (19.0)	42.2 (42.3)	3.6 (3.5)	c	2 070s, 2 060s	1 640m	
(14) [BaL ² (ClO ₄) ₂]	White	12.4 (12.3)	35.1 (35.2)	3.5 (3.2)	212		1 635m	1 130, 1 100, 1 050vs, 627, 625, 618ms
(15) [MnL ² (NCS) ₂ ·2MeOH]	Yellow	19.1 (19.1)	49.6 (49.6)	4.7 (5.2)	90	2 085 (sh), 2 075s	1 642m	
(16) [Co ₂ L ² (NCS) ₄]	Light brown	19.1 (19.6)	40.8 (40.3)	3.0 (3.1)	c	2 090ms, 1 985vs	1 628w	
(17) [Ni ₂ L ² (NCS) ₄]	Green	20.3 (20.1)	41.4 (41.4)	3.4 (3.2)	c	2 105ms, 1 985vs	1 623m	
(18) [Ni ₂ L ² (NCS) ₂ (MeCN) ₂ - (BPh ₄) ₂]	Green	10.6 (10.8)	68.2 (68.2)	5.3 (5.3)	152	1 975vs	1 627mw	740, 713ms
(19) [Cu ₂ L ² (NCS) ₂ (ClO ₄) ₂]	Green	14.0 (14.2)	33.5 (33.5)	3.0 (2.8)	c	2 070s	1 625mw	1 090vs, 629ms
(20) [Cu ₂ L ² (NCS) ₂ (BPh ₄) ₂]	Green	9.2 (9.1)	68.3 (68.4)	5.0 (5.1)	170	2 029s	1 623mw	740, 715ms
(21) [Cu ₂ L ² (N ₃) ₂ (ClO ₄) ₂]	Green	21.7 (22.2)	32.0 (31.7)	2.8 (2.9)	356	2 075s, 1 340ms ^d	1 623mw	1 090vs, 628ms
(22) [Cu ₂ L ² (OH)(ClO ₄) ₃]	Pale blue	10.5 (10.6)	30.5 (30.5)	3.1 (2.9)	409		1 630m	1 165, 1 091vs, 623ms
(23) [Cu ₂ L ³ (OH)(NCS) ₃ ·2H ₂ O]	Green	14.2 (14.4)	37.3 (37.1)	3.3 (3.7)	c	2 091s, 1 994ms	1 632ms	
(24) [Cu ₂ L ³ (NCS) ₄]	Ox-blood	15.8 (16.4)	38.9 (38.6)	3.2 (3.0)	c	2 086s, 1 952vs	1 632ms	

^a Calculated values in parentheses. ^b In *ca.* 10⁻³ mol dm⁻³ MeCN solution. ^c Insoluble. ^d $\nu_{\text{sym}}(\text{N}_3^-)$.

conformation (Figure 3) allows the co-ordinated metal ions to lie within reach of one >NCS bridge, a second intermediate NCS⁻ remaining unco-ordinated. The preference of Ni²⁺ for six-co-ordination ensures that no NCS⁻ ligand is left unco-ordinated in complex (8). The absorption at 2 090 cm⁻¹ could correspond either to N-terminal or N,S bridging (modes A or C) but molecular mechanics calculations make intramolecular bridging seem unlikely. With the smallest ion, Cu²⁺, it appears that no NCS-N bridge is possible within the L¹ cavity. On this reasoning, it would seem that the >NCS bridging mode might be favourable also in the case of Zn^{II} whose ionic radius approximates to that of Co^{II}, and indeed $\nu_{\text{asym}}(\text{NCS})$ absorption < 2 000 cm⁻¹ was observed for some preparations of (13), although the most satisfactory analyses were obtained with the all-N-terminal product.

The azide ion, N₃⁻, is well known^{17,18} to adopt a bridging mode through one terminal N when the intermetallic separation is necessarily short, which prompted the preparation of azido complexes (7), (11), and (21). There is no well defined i.r. criterion to distinguish azido-N and -N,N' bridging modes; one which has been used with varying degrees of success is the intensity with which the symmetric stretch, ν_{sym} (i.r.-silent in the free ion) appears in the i.r. spectrum. For $\mu\text{-N}_3\text{-N,N'}$ complexes this mode is likewise expected to be inactive or at least very weak. All three bis azido complexes, (7), (11), and (21), exhibit $\nu_{\text{sym}}(\text{N}=\text{N}=\text{N}^-)$ as a medium/weak absorption (superimposed on a weak macrocyclic ligand band). Coupled with the observation of $\nu_{\text{asym}}(\text{N}=\text{N}=\text{N}^-)$ at the high-frequency end of the normal range¹⁹ and other, e.g. e.s.r. evidence this constitutes a case for $\mu\text{-N}$ co-ordination of azide in these

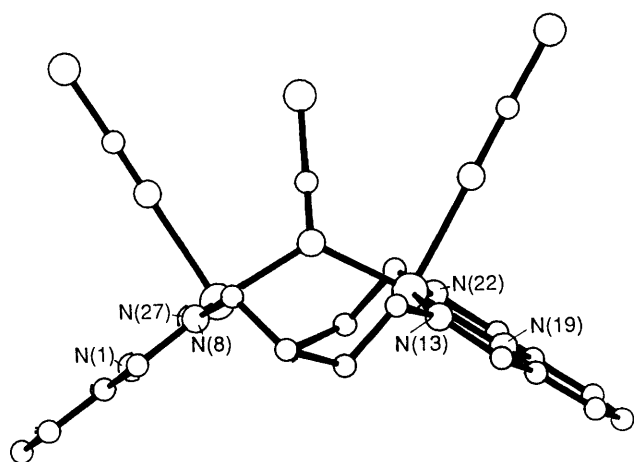


Figure 3. Structure of $[M_2L^1(NCS)_3]^+$ as predicted by molecular mechanics

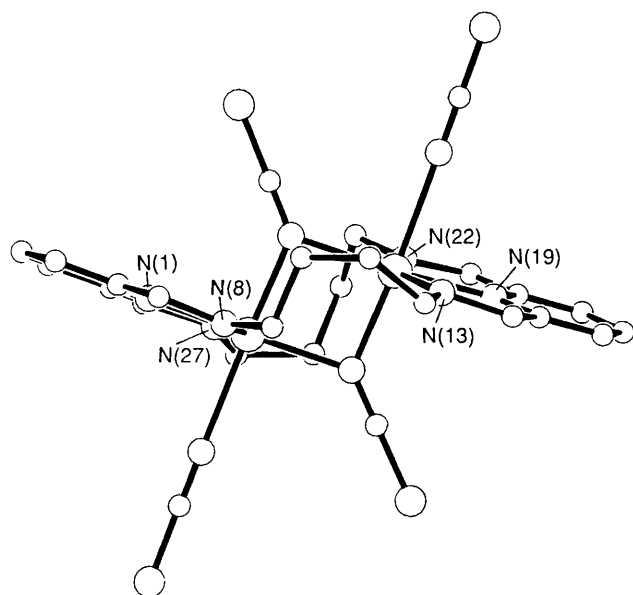


Figure 4. Structure of $[M_2L^1(NCS)_4]$ as predicted by molecular mechanics

complexes. The recent¹⁶ structure determination of (7) confirms this mode.

The other single-atom bridged L^1 complex in Table 4 is the dicopper(II) μ -hydroxo compound (12), for which this bridging mode is confirmed by e.s.r. spectroscopy (see later).

In the L^2 series, using once more the i.r. criterion, $>NCS$ bridging is seen to occur in the cobalt(II) and nickel(II) tetrathiocyanato complexes (16) and (17). Comparison of intensity of the i.r. absorption at $>2000\text{ cm}^{-1}$ with that of (3) indicates that here a pair of $>NCS$ bridges exist. Cavity size in this 20-membered macrocycle seems to offer a good fit for the

$\begin{array}{c} \text{N} \\ \diagup \quad \diagdown \\ \text{M} \quad \text{N} \\ \diagdown \quad \diagup \\ \text{N} \end{array}$ assembly in the case of these smaller transition-series

ions, the macrocycle presumably adopting the parallel-planar configuration (Figure 5). Complex (18) exhibits only a single, very strong, $\nu_{\text{asym}}(\text{NCS})$ absorption at 1975 cm^{-1} , which clearly originates in the di- μ -NCS- N assembly.

With L^2 and the larger transition-series ions Mn^{2+} and Fe^{2+} we were unable to isolate binuclear complexes of acceptable purity. With Mn^{II} the mononuclear complex (15) was obtained

no matter what excess of metal ion was used in the transmetalations. With Fe^{II} poorly characterised and non-reproducible products resulted, which did however display $\nu_{\text{asym}}(\text{NCS})$ i.r. absorption below 2000 cm^{-1} .

We obtained bis(thiocyanato) dicopper(II) L^2 complexes with perchlorate (19) and tetraphenylborate (20) counter ions. For (19) the single strong i.r. absorption at 2070 cm^{-1} points to terminal $-NCS$ co-ordination, but the single strong absorption at 2029 cm^{-1} for (20) cannot readily be so explained. Conductivity data rule out ionic thiocyanate, so it seems possible that complex (20) contains at least a weak $>N$ -only bridge. E.s.r. evidence (see Figure 8) does appear to support this idea.

In an attempt to reduce the cavity length to a value more suitable to the $Cu-N(\text{CS})-Cu$ assembly we then used the macrocycle L^3 .²⁰ Although 20-membered like L^2 , this offers a different copper co-ordination environment and a shorter internuclear distance. While transmetalation with Cu^{II} and excess of NCS^- in alcohol solution results²⁰ in the formation of a di- μ -alkoxy dicopper(II) complex with terminal $-NCS$ ligands, we were able to isolate $>NCS$ bridged products by carrying out the transmetalation at -20°C in dry acetonitrile. The i.r. criterion (Figure 6) indicates one $>NCS$ bridge for the tris(thiocyanato) derivative (23) and a pair of such bridges for the tetrakis derivative (24). We believe these compounds to be the first examples of truly symmetric $>NCS$ bridging between copper(II) ions. A recent²¹ report of N-only bridging describes a dimer with one $Cu-N$ distance of 1.92 and another of 3.05 \AA . Not surprisingly, perhaps, this dimer fails to conform to the i.r. criterion for $>NCS$ bridging, showing no $\nu_{\text{asym}}(\text{NCS})$ absorption below 2070 cm^{-1} .

Electronic and Magnetic Susceptibility Data.—Table 5 lists electronic spectral and magnetic data for L^1 , L^2 , and L^3 complexes. In lieu of conductivity measurements on the mainly very insoluble thiocyanato-complexes we have to rely on such data (in conjunction with i.r. data already discussed) to provide information on the co-ordination number as well as the geometry.

No absorption attributable to $d-d$ transitions was observed in the electronic spectra of complexes of Mn^{II} or Fe^{II} [although (4) showed the pair of intense charge-transfer absorptions often observed²² for pyridyl bis(imino) complexes of Fe^{II}]. As already discussed, i.r. spectra indicate six-co-ordination for Mn^{II} in (2), (3), and (15) and five-co-ordination for Fe^{II} in (4).

The dicobalt(II) complexes (5)–(7) and (16), all show three or four bands corresponding to $d-d$ absorption. For (6) and (7) a pair of absorptions close to 9500 and 16700 cm^{-1} are of appropriate frequency and intensity to be assigned to two of the three absorptions expected for Co^{II} in approximately octahedral geometry, reinforcing i.r. and magnetic evidence in support of six-co-ordination. (A third absorption above 20000 cm^{-1} appearing as a shoulder on a ligand absorption may correspond to the third $d-d$ transition.) On the other hand, the dominant feature of the electronic spectrum of complex (5) and the green form of (6) is a strong band around 15600 cm^{-1} , responsible for the green colour of the complexes. There are also broad weak features around 8500 and 7000 cm^{-1} poorly defined in the mull spectrum (which is all that is available for these very insoluble compounds). A similar spectrum has been observed¹⁵ for a structurally characterised square-pyramidal cobalt(II) complex, and indeed i.r. and magnetic data for (5) favour five-co-ordination.

The Nujol mull spectrum of complex (16) consists of a series of ill defined shoulders more reminiscent of trigonal bipyramidal Co^{II} than a regular octahedral geometry despite the co-ordination number of at least six which the i.r. spectrum requires for this complex. The observed magnetic moment may also suggest a low-symmetry environment for Co^{II} as, in the

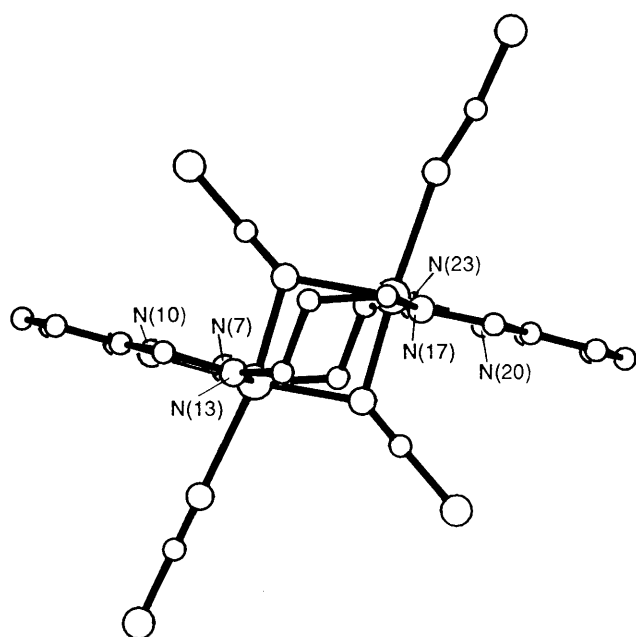


Figure 5. Structure of $[M_2L_2(NCS)_4]^+$ as predicted by molecular mechanics

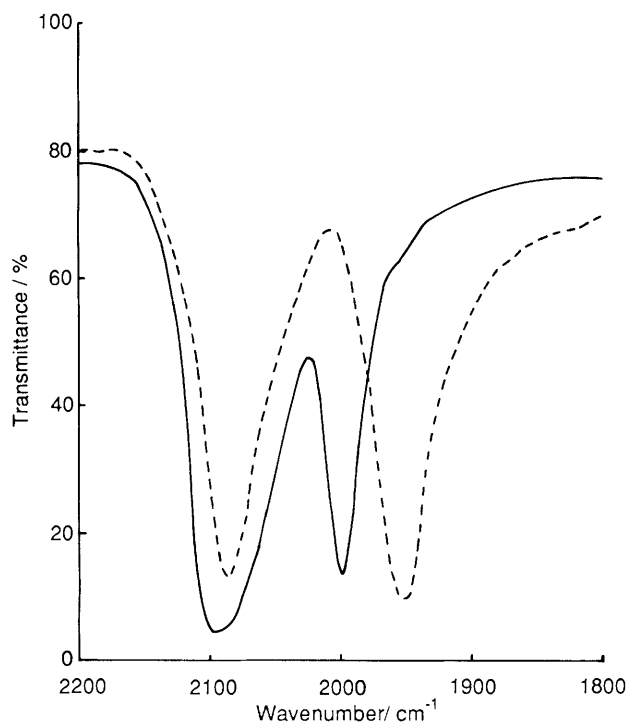


Figure 6. Infrared spectrum of complexes (23) (—) and (24) (---) over the 2200–1800 cm^{-1} range (KBr disk)

absence of significant antiferromagnetic interaction, the low moment could be interpreted as arising from a reduced orbital contribution.

Dinickel complexes (8), (17), and (18) show the expected three absorptions corresponding to the three allowed transitions for Ni^{II} in approximate O_h geometry, which accords with i.r. spectral evidence of six-co-ordination.

Of the dicopper(II) complexes only (23) shows the well defined splitting of the electronic transition which is associated²⁰ with D_{3h} symmetry. The absence of the splitting elsewhere in the series infers that for the remaining dicopper(II)

complexes square-based geometry (tetragonal or square pyramidal) applies. We are unable to explain the reason for the red-brown colour of complex (24). The Nujol mull electronic spectrum is broad and poorly defined with a broad tail which extends from the ligand $\pi-\pi^*$ absorption right through the visible; there are broad shoulders around 20 000, 25 000, 10 500, and 8 500 cm^{-1} some of which may be charge transfer in origin.

Magnetic Interactions.—Because the $>\text{NCS}$ mode of bridging paramagnetic ions is magnetically unexplored, it is of interest to establish its efficiency in the mediation of magnetic interaction. According to the Kahn theory,²³ spin polarisation by the delocalised π system of the bridging ligand can be expected to be responsible for the development of like spins on the magnetic orbitals of the pair of linked metal ions, hence leading to ferromagnetic interaction. This theory has been tested on the rather small number of structurally characterised^{24,25} di-azido-*N*-bridged dimers where indeed ferromagnetic interaction is observed. However, it must be noted that the distinction of ferromagnetic interaction from normal Curie-law behaviour in dicopper(II) systems is not always clear-cut, and some authors²⁶ have cast doubt on the validity of classifying interactions in such systems as ferromagnetic, in the absence of careful measurements down to very low (*i.e.* 1 K) temperatures.

We have examined the magnetic susceptibility of our transition-metal dimers initially over the temperature range 293–93 K, as shown in Table 5. Where significant interaction was indicated, the investigation was extended to cover the 93–4 K range. In the L^1 series the dimanganese(II) complexes (2) and (3) gave temperature-independent moments, close to the spin-only value, while the dicobalt(II), di-iron(II), and dinickel(II) complexes (4)–(6) and (8) showed no more than the expected²⁷ small reduction of moment with decreasing temperature, explained on the basis of depopulation of spin-orbit coupled excited states and/or zero-field effects. As described elsewhere,¹⁶ compound (7) shows an appreciable increase in moment with temperature over the 293–93 K range, which continues in the 93–4 K range achieving the plateau characteristic of a molecular ferromagnet, before falling off at low temperatures presumably because of antiferromagnetic interdimer interaction. Thus the spin-polarisation theory appears to hold quite satisfactorily for this μ -azido-*N* complex; however, there is no evidence of ferromagnetic interaction of comparable importance in the $>\text{NCS}$ -bridged dicobalt(II) complexes (5) and (6).

In the dicopper(II) L^1 series the pair of compounds (9) and (10) show the usual³ small reduction in moment with decreasing temperature corresponding to weak antiferromagnetic interaction revealed by e.s.r. spectra. With compound (11), despite the observation of well defined triplet features in the low-temperature e.s.r. spectrum, no reduction in moment over the range 293–93 K is observed, and we are inclined to attribute this behaviour to the existence of a spin-triplet ground state, as expected on the Kahn spin-polarisation model. The remaining dicopper(II) L^1 complex investigated, (12), shows moderately strong antiferromagnetic interaction (Table 6) mediated by the single hydroxo-bridge. The temperature dependence of the magnetic susceptibility can be fitted (Figure 7) by the Bleaney–Bowers equation (1), with $2J = -311 \text{ cm}^{-1}$ (assuming a 4%

$$\chi_m = \frac{Ng^2\beta^2}{3kT} [1 + \frac{1}{3} \exp(-2J/kT)]^{-1} + N\alpha \quad (1)$$

paramagnetic impurity). This compares with $2J$ values in the range -60 ²⁵ to $-1\,000 \text{ cm}^{-1}$ ²⁸ for other mono- μ -hydroxo-dicopper(II) complexes of known structure. The best match²⁹ of the exchange parameter J is at -161 cm^{-1} for a bipy dicopper(II) dimer with a $\text{Cu}(\mu\text{-OH})\text{Cu}$ angle of *ca.* 141.6° and $\text{Cu} \cdots \text{Cu}$ distance 3.645 Å.

Table 5. Electronic spectral and magnetic susceptibility data for dimeric complexes of L¹, L², and L³

Compound	<i>d-d</i> Bands ^a		μ /B.M.	
	Nujol Mull	MeCN solution ^b	293 K	93 K
(2) [Mn ₂ L ¹ (NCS) ₄]	—	—	6.05	6.09
(3) [Mn ₂ L ¹ (OMe)(NCS) ₃]	—	—	6.13	6.11
(4) [Fe ₂ L ¹ (NCS) ₄]·H ₂ O	21 000s, ^c 16 900s ^c	<i>d</i>	5.12	5.04
(5) [Co ₂ L ¹ (NCS) ₄]	17 200w (sh), 15 600ms, 8 980w, 7 400w (sh)	<i>d</i>	4.75	4.60
(6) [Co ₂ L ¹ (NCS)(MeCN) ₄ -(ClO ₄) ₃]	ca. 22 000 (sh), 16 400mw, 9 500w	22 000 (sh), 17 200(10), 9 090 (4.5)	5.08	4.98
(7) [Co ₂ L ¹ (N ₃) ₂ (MeCN) ₂ -(ClO ₄) ₂]	ca. 22 000 (sh), 17 000m, 9 500w	21 500 (sh), 17 500 (80), 9 600 (16)	5.24	5.57
(8) [Ni ₂ L ¹ (NCS) ₄]·H ₂ O	ca. 23 000 (sh), 14 900mw, 9 800mw	<i>d</i>	3.17	3.11
(9) [Cu ₂ L ¹ (NCS) ₄]	13 500ms	<i>d</i>	1.76	1.72
(10) [Cu ₂ L ¹ (NCS) ₂ (ClO ₄) ₂]	14 000ms	13 700 (450)	1.84	1.76
(11) [Cu ₂ L ¹ (N ₃) ₂ (ClO ₄) ₂]	15 900 (sh), 12 500ms	12 410 (350)	1.89	1.89
(12) [Cu ₂ L ¹ (OH)(ClO ₄) ₃]	13 300ms	13 300 (200)	1.42	0.46
(16) [Co ₂ L ² (NCS) ₄]	ca. 25 000 (sh), 17 000w (sh), 15 000 (sh), 8 500w	<i>d</i>	4.63	4.30
(17) [Ni ₂ L ² (NCS) ₄]	ca. 23 500 (sh), 16 300w, 10 100mw	<i>d</i>	3.11	3.10
(18) [Ni ₂ L ² (NCS) ₂ (MeCN) ₂ -(BPh ₄) ₂]	ca. 26 000(sh), ca. 17 200w, 10 900mw	ca. 24 000 (sh), 16 900 (32), 10 530 (90)	3.18	2.95
(19) [Cu ₂ L ² (NCS) ₂ (ClO ₄) ₂]	14 700ms	14 420 (420)	1.67	1.51
(20) [Cu ₂ L ² (NCS) ₂ (BPh ₄) ₂]	15 100ms	14 050 (400)	1.71	1.70
(21) [Cu ₂ L ² (N ₃) ₂ (ClO ₄) ₂]	14 800ms	14 200 (300)	1.85	1.85
(22) [Cu ₂ L ² (OH)(ClO ₄) ₃]	13 900ms	15 900 (sh), 13 300 (152)	1.60	0.90
(23) [Cu ₂ L ³ (OH)(NCS) ₃]·2H ₂ O	13 760, 9 800	<i>d</i>	1.84	1.84
(24) [Cu ₂ L ³ (NCS) ₄]	ca. 25 000br (sh), 10 500br (sh), 8 500br (sh)	<i>d</i>	1.89	1.85

^a v/cm⁻¹. ^b ε/dm³ mol⁻¹ cm⁻¹ in parentheses. ^c Charge-transfer bands. ^d Insoluble.

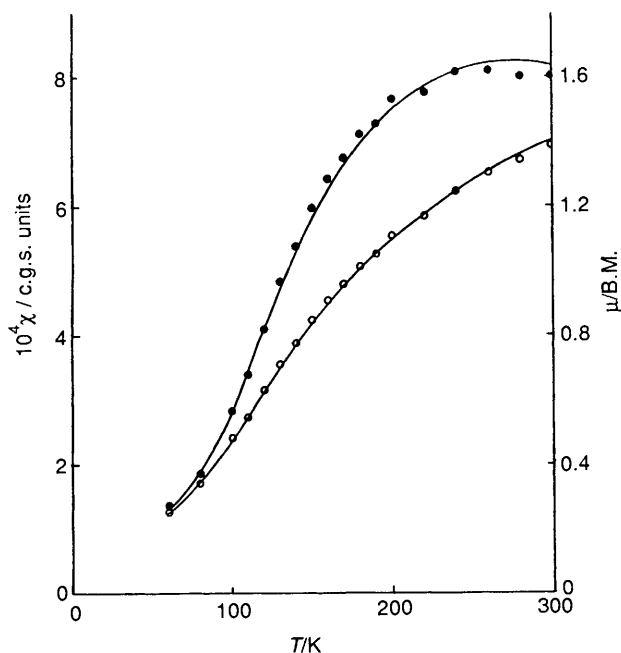


Figure 7. Temperature variation of the magnetic susceptibility of χ (●) and magnetic moment μ (○) of complex (12); symbols represent experimental points (c.g.s. = S.I. $\times 10^6/4\pi$)

In the L² series there is evidence of stronger interaction through the $>$ NCS bridge. However, this does not seem, with the possible exception of some dicopper(II) complexes, to be in the ferromagnetic sense. Moderately strong antiferromagnetic exchange appears to operate in complex (22) through the single hydroxo-bridge, but the temperature dependence of the susceptibility fails to conform to the Bleaney–Bowers equation (1). Either a sizeable fraction of paramagnetic impurity or a complex combination of intra- and inter-molecular exchange may

be invoked to explain this failure. The higher-than-expected low-temperature susceptibility is consistent with the appearance of a moderately strong, broad, signal around $g = 2.0$ in the e.s.r. spectrum which intensifies at low temperature at the expense of the triplet spectrum [Figure 8(b)]

The notionally unbridged dicopper(II) complex (19) shows moderately weak antiferromagnetic interaction as judged by the moments at 293 and 93 K and also by the observation of thermally accessible triplet features in the e.s.r. spectrum. Susceptibility values in the 4–80 K range are significantly higher than anticipated on the basis of an interacting dimer with a room-temperature moment of 1.67 B.M.; thus the Bleaney–Bowers equation is not obeyed. Of the remaining $>$ N bridged dicopper(II) complexes, (20), (21), (23), and (24) fail to show significantly reduced moments at 293 or 93 K, and this combined with the observation [in (20), (21), and (23)] of well defined triplet features in the e.s.r. spectrum [Figure 8(a)], leaves these three as candidates for weak ferromagnetic interactions of the kind postulated by Kahn. In contrast, (24) which shows good Curie–Law behaviour over the whole 4–300 K range has an e.s.r. spectrum which lacks triplet features.

Reasonably good fit with equation (1) can be achieved over the 4–300 K range for complexes (20), (21), and (23) using the small values of $-2J$ shown in Table 6; however it is also possible to consider the magnetic behaviour of (21) and (23) as a combination of ferromagnetic intra- and antiferromagnetic inter-dimer interaction. In Table 6, best-fit parameters over the range 4–300 K and also over the high-temperature range 100–300 K, where inter-dimer interactions are expected to be insignificant, are presented to cover these alternative explanations.

The absence of interactions between the paramagnetic centres in (24) is remarkable, given that the Cu...Cu distance must be of the order of 3.6–3.2 Å. The explanation may lie in a fortuitous cancellation of ferro- and antiferro-magnetic contributions.

E.S.R. Spectra of the Dicopper(II) Complexes.—Given the sensitivity of the e.s.r. technique to long-range interaction

Table 6. Dicopper(II) complexes: e.s.r. spectral data and magnetic exchange parameters (dimethylacetamide glass)

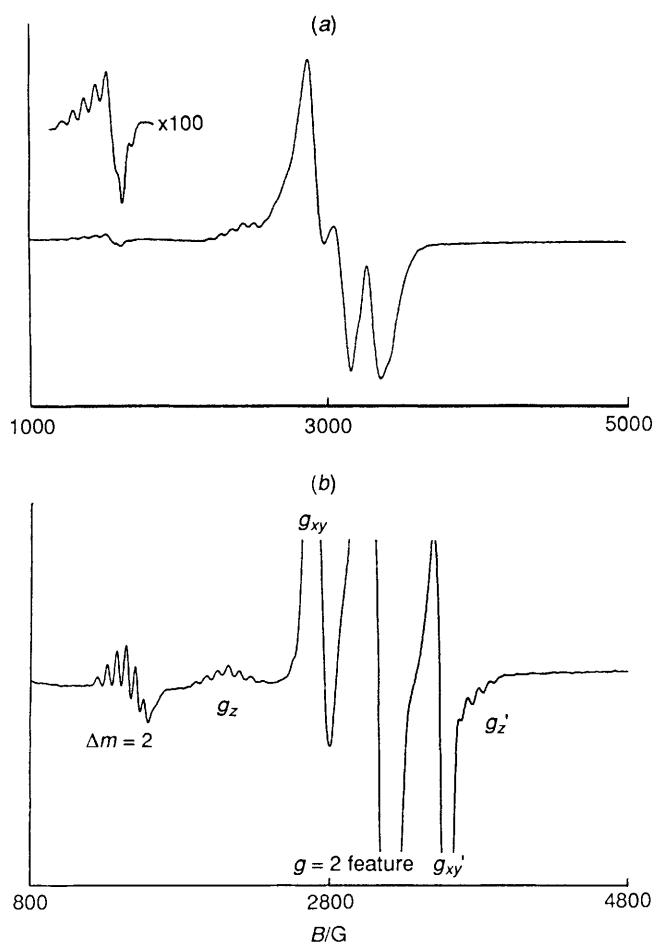
Compound	E.s.r.						$\Delta m = 2$ transition.		Magnetic exchange parameters					
	g_z	g_z'	g_z^{av}	D_z/G	A_z/G	$g_{x,y}$	$g_{x,y}'$	$g_{x,y}^{av}$	$D_{x,y}/G$	h.f.s./G	Rel. intensity ^a	$2J/cm^{-1}$	g	$N\alpha/10^{-6}$ c.g.s. units
(10) $[Cu_2L^1(NCS)_2(CIO_4)_2]$	2.45	2.20 ^b	2.33 ^b	150 ^b	67	2.18	1.98	2.08	290	63	1/20	-34 ^c	2.12	100
(11) $[Cu_2L^1(N_3)_2(CIO_4)_2]$	2.66	<i>b</i>	<i>b</i>	<i>b</i>	<i>d</i>	2.26	1.91	2.08	530	52	1	+8 ^c	2.10	100
(12) $[Cu_2L^1(OH)(CIO_4)_3]$	2.46	<i>b</i>	<i>b</i>	<i>b</i>	70	2.18	1.97	2.07	320	67	1/20	-311	2.05	120
(19) $[Cu_2L^2(NCS)_2(CIO_4)_2]$	2.61	<i>b</i>	<i>b</i>	<i>b</i>	77	2.24	1.92	2.08	490	80	1/2	<i>e</i>	<i>e</i>	<i>e</i>
(20) $[Cu_2L^2(NCS)_2(BPh_4)_2]$	2.63	<i>b</i>	<i>b</i>	<i>b</i>	75	2.25	1.91	2.08	510	73	1	+2	2.02	100
(21) $[Cu_2L^2(N_3)_2(CIO_4)_2]$	2.37	<i>b</i>	<i>b</i>	<i>b</i>	ca. 90 ^f	2.27	1.92	2.09	520	70	<i>b</i>	+7 ^c	2.08	120
(22) $[Cu_2L^2(OH)_2(CIO_4)_3]$	3.04	1.75	2.22	800	77	2.43	1.80	2.11	950	67	1	<i>e</i>	<i>e</i>	<i>e</i>
(23) $[Cu_2L^3(OH)(NCS)_3]^g$	<i>b</i>	<i>b</i>	<i>b</i>	<i>b</i>	<i>d</i>	2.40	2.10	2.20	550	<i>d</i>	<i>b</i>	+10 ^c	2.05	120
(24) $[Cu_2L^3(NCS)_4]^g$	<i>h</i>	<i>h</i>	2.27	<i>h</i>	ca. 160 ^f	<i>h</i>	<i>h</i>	2.04	<i>h</i>	<i>h</i>	<i>h</i>	or -4	2.15	120
												1	2.12	100

^a Peak height relative to g_z signal. ^b Estimation difficult because of overlapping. ^c In range 80–300 K. ^d Unresolved. ^e Poor fit by equation (1). ^f Broad, poorly resolved. ^g Insoluble; polycrystalline spectrum only. ^h No triplet features observed.

Table 7. Atomic co-ordinates ($\times 10^4$) for complex (1) with estimated standard deviations (e.s.d.s) in parentheses

Atom	x	y	z	Atom	x	y	z
Ba	5 000*	-2 722(1)	3 763(1)	C(21)	6 491(27)	-3 674(24)	2 109(13)
N(1)	5 462(14)	-3 260(14)	5 292(9)	N(22)	6 762(15)	-3 312(17)	2 789(12)
C(2)	6 517(18)	-3 214(18)	5 600(12)	C(23)	7 911(26)	-3 621(22)	3 043(20)
C(3)	6 869(25)	-3 725(19)	6 203(13)	C(24)	8 612(42)	-2 483(56)	3 064(24)
C(4)	6 022(28)	-4 226(21)	6 674(16)	C(25)	8 050(24)	-1 551(39)	3 303(24)
C(5)	4 943(35)	-4 319(19)	6 403(9)	C(26)	7 975(28)	-1 598(24)	4 220(22)
C(6)	4 725(19)	-3 828(18)	5 738(13)	N(27)	7 185(13)	-2 339(13)	4 509(11)
C(7)	3 544(18)	-3 888(20)	5 354(18)	C(28)	7 407(20)	-2 589(16)	5 183(17)
N(8)	3 312(17)	-3 493(12)	4 782(12)	Cl(3)	5 152(10)	-5 418(3)	3 698(4)
C(9)	2 135(16)	-3 556(27)	4 489(17)	O(31)	4 226(18)	-4 806(13)	3 390(13)
C(10)	1 404(15)	-2 649(17)	4 611(18)	O(32)	5 867(18)	-4 732(13)	4 084(12)
C(11)	1 829(17)	-1 804(20)	4 179(18)	O(33)	4 616(21)	-6 099(20)	4 233(17)
C(12)	1 883(27)	-1 631(25)	3 391(17)	O(34)	5 693(33)	-5 909(27)	3 121(17)
N(13)	2 872(29)	-2 170(21)	3 035(17)	Cl(2)	4 889(10)	207(3)	3 767(3)
C(14)	2 717(34)	-2 672(27)	2 399(27)	O(21)	3 787(18)	578(19)	3 980(14)
C(15)	3 525(23)	-3 201(20)	1 886(18)	O(22)	5 443(29)	839(26)	3 242(19)
C(16)	3 255(33)	-3 628(25)	1 179(16)	O(23)	4 603(26)	-649(23)	3 287(18)
C(17)	4 047(39)	-4 040(22)	823(21)	O(24)	5 508(38)	-179(39)	4 359(21)
C(18)	5 151(47)	-4 090(18)	1 065(14)	O(25)	5 139(39)	717(31)	3 072(19)
N(19)	4 564(17)	-3 233(12)	2 169(13)	O(26)	4 820(37)	-782(20)	3 810(22)
C(20)	5 425(27)	-3 679(16)	1 773(15)	O(27)	5 673(29)	584(33)	4 335(20)

* Parameter fixed.

**Figure 8.** Triplet features in dicopper(II) complexes as dimethylacetamide glasses: (a) (20) at 130 K; (b) (22) at 20 K.

between copper(II) ions, it is not surprising that all the dicopper(II) complexes in this study to some extent exhibit triplet features arising from the $S = 1$ state present either as a

ground or thermally accessible excited state. The features expected³⁰ include: (i) a hyperfine coupling constant $A_{\parallel}(\text{Cu})$, at ca. 80 G, around half the normal value of 140–160 G; (ii) anisotropy in the polycrystalline or glass spectrum arising from zero-field splitting, generating for the normal axial symmetry site two g_z and two $g_{x,y}$ signals, separated by zero-field splittings $2D_z$ and $D_{x,y}$ respectively, and (iii) the appearance with appreciable intensity of the normally forbidden half-band $\Delta m = 2$ transition, close to $g = 4$.

As Table 6 shows, for all the dicopper(II) complexes where solubility permits the acquisition of glass spectra, $A_{\parallel}(A_z)$ has a value close to 70 G showing that the unpaired electron is delocalised over both copper(II) sites. Where zero-field splittings are small, extensive overlapping of signals occurs in the X-band spectrum, making assignment of the high-field hyperfine-split g_z' signal difficult, although it is usually possible to identify with some confidence the pair of relatively sharp $g_{x,y}$ signals. This means that at least the $D_{x,y}$ zero-field parameter is available, and the magnitude of this offers some information on the degree of interaction between the paramagnetic centres. As the pseudo-dipolar zero-field splitting, D_{pseudo} ,³¹ involving excited-state superexchange can make an appreciable contribution to interaction in e.s.r. spectra, an exact correlation between the purely ground-state parameter, $2J$, obtained from magnetic susceptibility measurements, and the zero-field parameters D_z or $D_{x,y}$ is not to be expected. However, it does seem reasonable to interpret large zero-field effects as the consequence of significant interaction with the possibility of either a triplet or singlet level as the ground state. Also, zero-field parameters of similar magnitude may be taken as evidence of a similar bridging environment between paramagnetic centres, and this reinforces our earlier suggestion that complexes (11) and (21) both contain the azido-*N* bridge. On this basis also we believe that the large zero-field splittings for (20) [Figure 8(a)] are incompatible with Curie-law behaviour (which is one possible interpretation of the magnetic results) and propose instead a ferromagnetic ground state for this compound. We wished to examine the e.s.r. spectrum of (23) and (24) for evidence of weak ferromagnetic interaction. These complexes could not be dissolved without decomposition but the polycrystalline spectrum allowed a distinction to be drawn between (23) which presented a broad, zero-field-split pattern and (24) which showed the much sharper

Table 8 Atomic co-ordinates ($\times 10^4$) for complex (2) with e.s.d.s in parentheses

Atom	x	y	z	Atom	x	y	z
Ba	0*	-2 852(1)	5 000*	N(13)	1 522(13)	-2 425(18)	4 201(14)
Cl(1)	1 301(3)	-5 308(4)	5 028(4)	C(14)	1 651(15)	-2 695(22)	3 279(17)
O(11)	1 159(14)	-6 538(19)	5 062(16)	C(15)	1 009(31)	-2 499(52)	2 507(34)
O(12)	741(10)	-4 897(14)	4 193(10)	C(16)	92(16)	-2 993(18)	2 278(18)
O(13)	1 083(11)	-4 771(14)	5 795(12)	N(17)	-388(13)	-2 698(15)	2 975(14)
O(14)	2 131(14)	-5 033(19)	5 053(16)	C(18)	-1 101(16)	-2 059(16)	2 505(18)
Cl(2)	-55(4)	185(3)	5 053(5)	C(19)	-1 703(13)	-1 606(17)	3 068(15)
O(21)	-310(9)	-550(13)	5 695(10)	N(20)	-1 642(12)	-1 938(15)	3 965(13)
O(22)	779(11)	747(16)	5 546(13)	C(41)	-2 348(15)	-912(23)	2 588(19)
O(23)	-681(11)	1 014(15)	4 710(12)	C(42)	-2 968(14)	-574(21)	3 107(17)
O(24)	130(11)	-483(15)	4 279(11)	C(43)	-2 901(13)	-900(17)	3 990(14)
N(7)	420(15)	-2 621(21)	7 116(15)	C(21)	-2 195(15)	-1 681(22)	4 435(17)
C(8)	895(16)	-2 052(17)	7 401(18)	C(22)	-2 156(13)	-2 062(15)	5 381(15)
C(9)	1 588(15)	-1 520(18)	6 997(16)	N(23)	-1 585(15)	-2 595(21)	5 773(15)
N(10)	1 512(10)	-1 840(15)	6 086(11)	C(24)	-1 665(17)	-3 087(25)	6 701(19)
C(11)	2 191(12)	-1 444(15)	5 687(14)	C(25)	-963(21)	-2 504(33)	7 561(22)
C(51)	2 791(14)	-738(19)	6 179(15)	C(26)	-158(20)	-3 236(30)	7 679(23)
C(52)	2 842(14)	-460(19)	7 088(15)	O(100)	-1 122(12)	-4 730(17)	4 854(14)
C(53)	2 215(17)	-863(27)	7 466(21)	C(101)	-1 123(24)	-5 807(38)	4 654(29)
C(12)	2 142(12)	-1 771(18)	4 749(13)	C(102)	-877(65)	-6 228(121)	5 201(84)

* Fixed parameters.

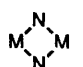
Table 9. Bond lengths (Å) involving the Ba atom in complexes (1) and (14)

(1)		(14)	
Ba-N(1)	2.832(16)	Ba-O(12)	3.061(16)
Ba-N(8)	2.867(21)	Ba-O(13)	2.943(17)
Ba-N(13)	2.912(33)	Ba-O(21)	3.005(15)
Ba-N(19)	2.926(22)	Ba-O(24)	3.036(18)
Ba-N(22)	2.803(20)	Ba-N(7)	2.973(22)
Ba-N(27)	2.936(17)	Ba-N(10)	2.835(16)
Ba-O(31)	2.976(17)	Ba-N(13)	2.981(19)
Ba-O(32)	2.903(18)	Ba-N(17)	2.837(19)
Ba-O(23)	2.903(30)	Ba-N(20)	2.922(18)
Ba-O(26)	2.575(27)	Ba-N(23)	3.024(23)
		Ba-O(100)	2.855(20)

parallel/perpendicular spectrum with poorly resolved *ca.* 160 G hyperfine splitting characteristic of non-interacting copper(II). Thus, the e.s.r. spectrum of complex (24) is consistent with its magnetic (Curie-law) behaviour while the magnetic results for (23) could be interpreted as deriving from weak ferromagnetic intradimer exchange, but the distinction from normal Curie-law behaviour is, as in all these dicopper(II) dimers, at the limits of significance.

Conclusion

Using the set of macrocyclic ligands L^1 , L^2 , and L^3 we have succeeded in obtaining $>$ NCS bridged dinuclear complexes of all five members of the first transition series from Mn^{II} to Cu^{II} .

The best fit for the  assembly is achieved for $M =$

Mn^{II} within the 22-membered macrocycle L^1 and for $M = Co^{II}$ or Ni^{II} within the 20-membered macrocycle L^2 , while the monobridged $M-N(CS)-M$ assembly occurs within L^1 for $M = Fe^{II}$, Co^{II} , and Ni^{II} . In order to ensure a good fit for either di- or mono- $>$ NCS bridges with dicopper(II), we have had to use the macrocycle L^3 which, because of the disposition of donor atoms, has a smaller effective cavity than L^2 . As the first examples of truly symmetric $>$ NCS bridging, the resultant tetrakis- and tris-(thiocyanato) dicopper(II) L^3 complexes are of some interest.

The $>$ NCS bridge does not appear to be an efficient mediator of magnetic interaction, in comparison with the fairly strong antiferromagnetic interaction transmitted *via* $\mu-OH^-$ or the weaker ferromagnetic interaction *via* $\mu-N_3-N$ in these systems. However, in two cases where $>$ NCS bridges linked copper(II) ions there is some evidence for weak ferromagnetic interaction, perhaps generated by a weak spin polarisation on the Kahn model. This cannot be a universal effect, as the compound which best fits the i.r. criterion for $>$ NCS bridging shows no evidence for the existence of a triplet ground state.

Experimental

Synthesis of the Ligands L^1 and L^2 .—2,6-Diformylpyridine was prepared, as described earlier³² by SeO_2 oxidation of pyridine-2,6-dimethanol purchased from Aldrich. To 2,6-diformylpyridine (7 mmol) dissolved in MeOH (*ca.* 200 cm^3) was added the appropriate diamine (6.5 mmol) and $Ba(ClO_4)_2$ (3 mmol). The reagents were stirred together overnight at room temperature, after which white crystals of $[BaL(ClO_4)_2]$ were filtered off, and the filtrate was evaporated to yield further crops of product. Yield *ca.* 65–75%.

The complex $[BaL^2(ClO_4)_2] \cdot EtOH$ for X-ray crystallographic structure determination was obtained by recrystallising (14) from MeCN-EtOH, $[BaL^3(ClO_4)_2] \cdot EtOH$ was prepared, as described earlier³³ by an analogous procedure.

Transmetallations.—Tetrathiocyanato complexes (2), (4), (5), (8), (9), (13), (16), and (17). These were prepared by transmetalation of the barium complex with the appropriate transition-metal perchlorate in the presence of excess of thiocyanate, typically as follows. The complex $[BaL(ClO_4)_2]$ (0.5 mmol) was dissolved in MeCN (50 cm^3) and the appropriate metal perchlorate (1 mmol) added, followed by reflux for *ca.* 30 min. Sodium thiocyanate (2–3 mmol) dissolved in EtOH (20 cm^3) was then added with stirring, and the mixture concentrated to *ca.* 30 cm^3 on a rotary evaporator before leaving to crystallise at $-20^\circ C$. Yields *ca.* 50–80%. Compounds (2) and (15) were the products of transmetalation when (1) and (14) respectively were treated with $Mn^{2+}-NaNCS$ (1:2) in MeOH solution.

Bis(thiocyanato) and bis(azido) diperchlorates (7), (10), (11), (19), and (21). The complex $[BaL(ClO_4)_2]$ (0.5 mmol) was dissolved in MeCN (250 cm^3) and the appropriate metal per-

chlorate (1 mmol) added. The mixture was stirred at reflux while a solution of NaNCS (1 mmol) in EtOH (50 cm³) or solid NaN₃ (1 mmol) was added. When all the solid has dissolved, the volume was reduced to ca. 50 cm³ and cooled to -20 °C to crystallise the desired product. Yields typically 30–50%.

Bis (and mono)-thiocyanato tetraphenylborate complexes, (18) and (20). The complex [BaL²(ClO₄)₂] (1 mmol) was dissolved in MeCN (250 cm³) and the appropriate metal perchlorate (2 mmol) added, followed by NaNCS in EtOH (50 cm³). Finally, excess of (>4 mmol) of solid sodium tetraphenylborate was added. Crystals of the desired product were obtained on reduction of the volume and cooling to -20 °C. Yields ca. 30–50%.

μ-Hydroxo-dicopper(II) perchlorates (12) and (22). To [BaL(ClO₄)₂] (1 mmol) suspended in alcohol (200 cm³) (MeOH for L = L¹, EtOH for L = L²) was added Cu(ClO₄)₂·6H₂O (4 mmol) and the mixture warmed to ca. 50 °C for 1 h. On cooling, the blue solid was filtered off. The complex [Cu₂L¹(OH)(ClO₄)₃] was recrystallised from MeCN–EtOH, but [Cu₂L²(OH)(ClO₄)₃] could not be recrystallised. Yields ca. 55%.

L³ Complexes: [Cu₂L³(OH)(NCS)₃] (23). To [Cu₂L³(OH)₂(ClO₄)₂]·H₂O (0.25 mmol) (prepared as described earlier³⁴) dissolved in freshly dried MeCN (30 cm³) at -20 °C was added NaNCS (0.1 mmol) in MeCN (10 cm³), also at -20 °C. A small amount of turbidity was filtered off and the solution left at -20 °C for >2 weeks to crystallise. Tiny bright green microcrystals were obtained in ca. 30% yield.

[Cu₂L³(NCS)₄] (24). The complex [BaL³(ClO₄)₂]·EtOH²⁰ (0.5 mmol) was dissolved in dry MeCN (30 cm³), and Cu(CF₃SO₃)₂ (1 mmol) was added. The solution was filtered and cooled to -20 °C, after which it was mixed with a solution of NaNCS (1 mmol) in dry MeCN (10 cm³) at -20 °C. After 1 d at -20 °C the orange-brown microcrystals were filtered off in ca. 40% yield. This product deteriorates within days of making unless stored under dry conditions at < -20 °C.

Physical Measurements.—Infrared spectra were measured as KBr discs or Nujol mulls using a Perkin-Elmer 983 G spectrophotometer, electronic spectra as MeCN solutions or Nujol mulls using a Perkin-Elmer λ9 spectrometer. Magnetic susceptibility measurements were made either by the Gouy method using a Stanton microbalance and Newport Instrument cryostat, or by the Faraday method using an Oxford Instruments resistive susceptibility system with liquid-helium flow cryostat. E.s.r. spectra were measured as X-band with a Varian E-109 spectrometer equipped with an Oxford Instruments continuous-flow cryostat.

X-Ray Structure Determinations.—Crystal data for complex (1). [BaL¹(ClO₄)₂], C₂₂H₂₆BaCl₂N₆O₈, M = 710.5, orthorhombic, space group P2₁cn [non-standard setting of Pn2₁ (no. 33)], a = 11.80(1), b = 13.22(1), c = 17.57(2) Å, U = 2 740.8 Å³, F(000) = 1 416, D_m = 1.74 g cm⁻³, Z = 4, D_c = 1.72 g cm⁻³, Mo-K_α radiation (λ = 0.7107 Å), μ(Mo-K_α) = 10.1 cm⁻¹.

Crystal data for complex (14). [BaL²(ClO₄)₂]·EtOH, C₂₂H₂₀BaCl₂N₆O₉, M = 742.5, monoclinic, space group Aa [non-standard setting of C_c (no. 9)], a = 16.074(15), b = 11.940(14), c = 14.381(14) Å, β = 103.5(1), U = 2 683.9 Å³, F(000) = 1 488, D_m = 1.77 g cm⁻³, Z = 4, D_c = 1.80 g cm⁻³, Mo-K_α radiation (λ = 0.7107 Å), μ(Mo-K_α) = 17.87 cm⁻¹.

2 719 Independent reflections [for (1)] and 2 734 [for (14)] with 2θ_{max} of 50° were measured on a diffractometer, of which 1 740 with I > 3σ(I) for (1) and 2 140 with I > 2σ(I) for (14) were used in subsequent calculations. In both structures the positions of the metal atoms were determined from the Patterson function. Remaining atoms were determined from Fourier maps. In (14) a solvent ethanol molecule was located.

In (1) one perchlorate was disordered and two tetrahedral arrangements of the oxygen atoms were refined each with half-occupancy.

In complex (1) the structure was refined [Ba, Cl, O (ordered perchlorate), C, all anisotropic; O (disordered perchlorate) isotropic, H isotropic in calculated positions] to R 0.074 (R' = 0.079). The structure with the signs of the co-ordinates reversed refined to R 0.075. In (14) the structure was refined [Ba, Cl, anisotropic; O, N, C, H (in calculated positions), isotropic] to R 0.080 (R' = 0.082). The structure with the signs of the co-ordinates reversed gave R 0.081.

Calculations were performed using full-matrix least-squares methods with a weighting scheme w = 1/[σ²(F) + 0.003F²]. The SHELX 76³⁵ program and some of our own programs were employed on the Amdahl V7 Computer at the University of Reading. Positional co-ordinates are given in Tables 7 and 8 and molecular dimensions in the metal co-ordination spheres are compared in Table 9.

Additional material available from the Cambridge Crystallographic Data Centre comprises H-atom co-ordinates, thermal parameters, and remaining bond lengths and angles.

Acknowledgements

We thank Dupont company and the Open University for a Matched-Fund studentship to (D. McD.). We also acknowledge the assistance of the Open University Research Committee in part-funding the Faraday balance and e.s.r. cryostat. Thanks are due to the S.E.R.C. for providing funds towards purchase of the Faraday balance, Perkin-Elmer λ9 spectrophotometer, and the diffractometer. We are grateful to Mr. A. Johans for assistance in obtaining the crystallographic data. D. McD. and J. N. are also affiliated to Queens University, Belfast.

References

- 1 K. D. Karlin and J. Zubieta (eds.), 'Biological and Inorganic Copper Chemistry,' Adenine Press, New York, 1985; S. F. Lippard, *Angew. Chem. Int., Ed. Eng.*, 1988, **47**, 344.
- 2 S. M. Nelson, *Inorg. Chim. Acta*, 1982, **62**, 39.
- 3 J. Nelson, B. P. Murphy, M. G. B. Drew, P. Yates, and S. M. Nelson, *J. Chem. Soc., Dalton Trans.*, 1988, 1001 and refs. therein.
- 4 J. L. Burmeister, in 'Chemistry and Biochemistry of Thiocyanic acid and its Derivatives,' ed. A. A. Newman, Academic Press, London, 1975.
- 5 K. Pohl, K. Wiegardt, B. Nuber, and J. Weiss, *J. Chem. Soc., Dalton Trans.*, 1987, 187.
- 6 M. B. Cingi, A. M. M. Lanfredi, A. Tiripicchio, J. G. Haasnoot, and J. Reedijk, *Inorg. Chim. Acta*, 1983, **72**, 81.
- 7 J. G. Haasnoot, W. L. Driessen, and J. Reedijk, *Inorg. Chem.*, 1984, **23**, 2803.
- 8 F. A. Cotton, A. Davidson, W. H. Isley, and H. S. Trop, *Inorg. Chem.*, 1979, **18**, 279.
- 9 G. A. van Albada, R. A. G. de Graaff, G. A. Haasnoot, and J. Reedijk, *Inorg. Chem.*, 1984, **23**, 1404 and refs. therein.
- 10 S. Raghunathan, C. Stevenson, J. Nelson, and V. McKee, *J. Chem. Soc., Chem. Commun.*, 1989, 5 and refs. therein.
- 11 N. L. Allinger and Y. H. Yuh, MM2 program, Q.C.P.E. Program No. 423, Quantum Chemistry Program Exchange, Indiana University Chemistry Department, Indiana, 1977, modified version 1980.
- 12 M. G. B. Drew and P. C. Yates, *J. Chem. Soc., Chem. Commun.*, 1987, 2563.
- 13 M. G. B. Drew, S. Hollis, and P. C. Yates, *J. Chem. Soc., Dalton Trans.*, 1985, 1829.
- 14 B. P. Murphy, J. Nelson, M. G. B. Drew, P. Yates, and S. M. Nelson, *J. Chem. Soc., Dalton Trans.*, 1987, 123.
- 15 F. Lions, I. G. Dance, and J. Lewis, *J. Chem. Soc. A*, 1967, 565.
- 16 C. J. Harding, J. Nelson, C. Stevenson, and M. G. B. Drew, unpublished work.
- 17 O. Kahn, S. Sikorav, J. Gouteron, S. Jeannin, and Y. Jeannin, *Inorg. Chem.*, 1983, **22**, 287.

- 18 T. N. Sorrell, in 'Biological and Inorganic Copper Chemistry,' eds. K. D. Karlin and J. Zubieta, Adenine, New York, 1986.
- 19 M. G. B. Drew, J. Nelson, F. S. Esho, V. McKee, and S. M. Nelson, *J. Chem. Soc., Dalton Trans.*, 1982, 1837.
- 20 M. G. B. Drew, P. C. Yates, F. S. Esho, J. T. Grimshaw, K. P. McKillop, S. M. Nelson, and J. Nelson, *J. Chem. Soc., Dalton Trans.*, 1988, 2995 and refs. therein.
- 21 J. L. Mesa, T. Jojo, M. Arriortua, G. Villeneuve, J. L. Folgado, A. B-Porter, and D. B-Porter, *J. Chem. Soc., Dalton Trans.*, 1989, 53.
- 22 M. F. Cabral, B. P. Murphy, and J. Nelson, *Inorg. Chim. Acta*, 1984, **96**, 169.
- 23 M. F. Charlot, O. Kahn, M. Chaillet, and C. Larrieu, *J. Am. Chem. Soc.*, 1986, **108**, 2574.
- 24 J. Coramond, P. Plumeré, J. M. Lehn, Y. Agnus, R. Louis, R. Weiss, O. Kahn, and I. Morgenstern-Badarau, *J. Am. Chem. Soc.*, 1982, **104**, 6330.
- 25 S. Sikorav, I. Bkouche-Waksman, and O. Kahn, *Inorg. Chem.*, 1984, **23**, 490.
- 26 See, for example, R. L. Carlin, 'Magnetochemistry,' Springer, New York, 1986.
- 27 A. Earnshaw, 'Introduction to Magnetochemistry,' Academic Press, London, 1968.
- 28 P. K. Coughlin and S. J. Lippard, *J. Am. Chem. Soc.*, 1981, **103**, 3228.
- 29 M. S. Haddad, S. R. Wilson, D. J. Hodgson, and D. N. Hendrickson, *J. Am. Chem. Soc.*, 1981, **103**, 384.
- 30 J. E. Wertz and J. R. Bolton, in 'Electron Spin Resonance,' Chapman and Hall, London, 1986, ch. 10.
- 31 T. R. Felthouse and D. N. Hendrickson, *Inorg. Chem.*, 1978, **17**, 444.
- 32 S. M. Nelson, C. W. Knox, M. McCann, and M. G. B. Drew, *J. Chem. Soc., Dalton Trans.*, 1981, 1669.
- 33 M. G. B. Drew, P. C. Yates, J. T. Grimshaw, A. Lavery, K. P. McKillop, S. M. Nelson, and J. Nelson, *J. Chem. Soc., Dalton Trans.*, 1988, 347.
- 34 M. G. B. Drew, F. S. Esho, A. Lavery, and S. M. Nelson, *J. Chem. Soc., Dalton Trans.*, 1984, 545.
- 35 G. M. Sheldrick, SHELX 76, Package for Crystal Structure Calculations, Cambridge University, 1976.

Received 19th July 1989; Paper 9/03063H